



UNIVERSITY OF LEEDS

This is a repository copy of *Quantifying the cellular uptake of semiconductor quantum dot nanoparticles by analytical electron microscopy*.

White Rose Research Online URL for this paper:  
<http://eprints.whiterose.ac.uk/84544/>

Version: Accepted Version

---

**Article:**

Hondow, N, Brown, MR, Starborg, T et al. (5 more authors) (2015) Quantifying the cellular uptake of semiconductor quantum dot nanoparticles by analytical electron microscopy. *Journal of Microscopy*. ISSN 0022-2720

<https://doi.org/10.1111/jmi.12239>

---

**Reuse**

Unless indicated otherwise, fulltext items are protected by copyright with all rights reserved. The copyright exception in section 29 of the Copyright, Designs and Patents Act 1988 allows the making of a single copy solely for the purpose of non-commercial research or private study within the limits of fair dealing. The publisher or other rights-holder may allow further reproduction and re-use of this version - refer to the White Rose Research Online record for this item. Where records identify the publisher as the copyright holder, users can verify any specific terms of use on the publisher's website.

**Takedown**

If you consider content in White Rose Research Online to be in breach of UK law, please notify us by emailing [eprints@whiterose.ac.uk](mailto:eprints@whiterose.ac.uk) including the URL of the record and the reason for the withdrawal request.



[eprints@whiterose.ac.uk](mailto:eprints@whiterose.ac.uk)  
<https://eprints.whiterose.ac.uk/>

## **Quantifying the cellular uptake of semiconductor quantum dot nanoparticles by analytical electron microscopy**

Nicole Hondow,<sup>1</sup> M. Rowan Brown,<sup>2</sup> Tobias Starborg,<sup>3</sup> Alexander G. Monteith,<sup>4</sup> Rik Brydson,<sup>1</sup> Huw D. Summers,<sup>2</sup> Paul Rees,<sup>2</sup> and Andy Brown<sup>1</sup>

Corresponding Author: Dr Nicole Hondow, Institute for Materials Research, School of Chemical and Process Engineering, University of Leeds, Leeds LS2 9JT, UK. n.hondow@leeds.ac.uk

1. Institute for Materials Research, School of Chemical and Process Engineering, University of Leeds, Leeds LS2 9JT, UK
2. Centre for Nanohealth, College of Engineering, Swansea University, Singleton Park, Swansea SA2 8PP, UK
3. Wellcome Centre for Cell Matrix Research, University of Manchester, Manchester M13 9PT, UK
4. Gatan UK, 25 Nuffield Way, Abingdon OX14 1RL, UK

### **Key words**

quantum dots, cellular uptake, nanoparticle dose, TEM, SBF SEM, EFTEM

### **Summary**

Semiconductor quantum dot nanoparticles are in demand as optical biomarkers yet the cellular uptake process is not fully understood; quantification of numbers and the fate of internalised particles are still to be achieved. We have focussed on the characterisation of cellular uptake of quantum dots using a combination of analytical electron microscopies because of the spatial resolution available to examine uptake at the nanoparticle level, using both imaging to locate particles and spectroscopy to confirm identity. In this study, commercially available quantum dots, CdSe/ZnS core/shell particles coated in peptides to target cellular uptake by endocytosis, have been investigated in terms of the agglomeration state in typical cell culture media, the traverse of particle agglomerates across U-2 OS cell membranes during endocytosis, the merging of endosomal vesicles during incubation of cells and in the correlation of imaging flow cytometry and TEM to measure the final nanoparticle dose internalised by the U-2 OS cells. We show that a combination of analytical TEM and serial block face SEM can provide a comprehensive description of the internalisation of an initial exposure dose of nanoparticles by an endocytically active cell population and how the internalised, membrane bound nanoparticle load is processed by the cells. We present a stochastic model of an endosome merging process and show that this provides a data driven modelling framework for the prediction of cellular uptake of engineered nanoparticles in general.

## Lay summary

Engineered nanoparticles offer potential for improved medical diagnosis and treatment. The particles are small enough to enter cells and we can monitor this process using electron microscopy. The microscopy provides the resolution to count numbers of nanoparticles internalised by cells so that we can know the exact dose received by a cell or cell population and the final fate of the nanoparticles.

## Introduction

The emerging field of nanomedicine centres on the design and use of nanoparticles with specific functions for biomedical applications (Kim *et al.*, 2010). Nanoparticles are strong candidates for drug delivery and imaging biomarkers (Koo *et al.*, 2005) because they are small enough to enter cells without necessarily disrupting function, especially if size, shape, surface-to-volume ratio, composition and surface chemistry are appropriately controlled (Doane & Burda, 2012). Despite the infancy of the field there are nearly 250 nanomedicine products approved or in various stages of clinical study (Etheridge *et al.*, 2013). Yet uncertainty remains as to the precise action and fate of many of these particles (De Jong & Borm, 2008).

One of the most promising nanoparticle types for optical biomarker applications are quantum dots: namely semiconductor crystals which when optically stimulated fluoresce at a wavelength dependent upon size, structure and composition. These nanoparticulate crystals have numerous advantages over traditional fluorophores including long-term stability, brightness and the capacity for functionalization by tailoring of surface chemistry (Brown *et al.*, 2010, Jamieson *et al.*, 2007, Michalet *et al.*, 2005, Wang & Chen, 2011). The semiconductor crystals often contain toxic elements such as cadmium however particle breakdown and release of toxic ions into the cellular environment can be inhibited by coating the core with a more stable and inert shell such as zinc sulphide (Jamieson *et al.*, 2007). Surface functionalization of the shell is then vital to enable cellular internalization to proceed through routine pathways such as endocytosis; a single quantum dot is large enough for multiple ligands to be attached to the particle surface (Wang & Chen, 2011) and specialist ligands are used to encourage cellular uptake, for example specific surface functionalization can enable receptor-mediated or non-specific endocytosis to dominate uptake (Jaiswal *et al.*, 2003, Michalet *et al.*, 2005).

The use of quantum dot nanoparticles as biomarkers is becoming well established for example, as labels to accurately track cell populations *in vitro* over 8 h timescales (Rees *et al.*, 2014). These applications demand a full understanding of the cellular uptake, including quantification of numbers and the fate of internalised particles. Characterisation of *in vitro* studies commonly includes electron microscopy where transmission electron microscopy (TEM) has the spatial resolution to examine cellular uptake at the nanoparticle level, using both imaging to locate particles and spectroscopy to confirm identity (Brown & Hondow, 2013, Elsaesser *et al.*, 2011). The latter can be essential to avoid analysing contrast-enhancing heavy metal staining artefacts (Mühlfeld *et al.*, 2007, Rothen-Rutishauser *et al.*, 2006). It is possible however to prepare samples via conventional preparation routes without post staining (*i.e.* fixation, dehydration, resin embedding and ultramicrotomy); permitting the identification of, for example, low contrast silica nanoparticles in

the cytoplasm of A549 cells with confirmation of composition provided by the analytical TEM techniques of energy dispersive X-ray (EDX) spectroscopy and energy filtered TEM (EFTEM) (Mu *et al.*, 2012).

In recent work we have focussed on the characterisation of cellular uptake of quantum dots using analytical electron microscopy. Commercially available quantum dots, CdSe/ZnS core/shell particles coated in arginine-rich peptides to target cellular uptake by endocytosis, have been investigated in terms of the agglomeration state in typical cell culture media (Hondow *et al.*, 2012), the traverse of particle agglomerates across U-2 OS cell membranes during endocytosis (Brown *et al.*, 2014) and in the correlation of imaging flow cytometry and TEM to measure the final nanoparticle dose internalised by the U-2 OS cells (Summers *et al.*, 2013). This comprehensive description of how an initial exposure dose of nanoparticles is internalised by an endocytically active cell population (whose cell cycle is not perturbed by these quantum dots (Errington *et al.*, 2010)) and how the internalised, membrane bound nanoparticle load is processed by the cells required correlation of thin-section TEM analysis to whole cell data.

Cells have been previously visualised in 3-D by electron tomography (Leis *et al.*, 2008) or by examining serial sections (White *et al.*, 1986) on the TEM; however, both of these are accompanied by disadvantages, including limited application to larger volumes, being labour-intensive and time consuming (Denk & Horstmann, 2004, Hughes *et al.*, 2013, Zankel *et al.*, 2009). An alternative, serial block face scanning electron microscopy (SBF SEM), allows the collection of 3-D data through the imaging of a resin block which is serially sectioned inside the chamber of an SEM (Denk & Horstmann, 2004). SBF SEM, which has been used extensively in the biological sciences and is also finding applications in materials sciences (Hashimoto *et al.*, 2013, Hughes *et al.*, 2013, Zankel *et al.*, 2009), is suited to the analysis of the cellular uptake of nanoparticles. An initial report conducted on the uptake of hydroxyapatite nanoparticles by human monocyte-macrophages has provided insight regarding incomplete nanoparticle internalisation, something that was not evident by TEM alone (Motskin *et al.*, 2011).

Electron microscopy of a cellular sample embedded in resin provides a fixed time point on which to conduct analysis. Whilst this may be perceived as a disadvantage when monitoring a dynamic biological process such as particle uptake, it does provide the opportunity for extensive examination at a resolution where individual nanoparticles can be identified and counted. TEM studies on cells fixed at different incubation time points enable inference of processes that may have occurred between the times, potentially with the opportunity of correlation to more continuous, bulk measures. The uptake of silica nanoparticles has been tracked from initial internalisation (after 4 h) to final sub-cellular localisation (after 24 h and 48 h) by examining TEM sections prepared at different times (Shapero *et al.*, 2011) and the crossing of intracellular membranes by modified gold nanoparticles has been studied by TEM at various time points (2 h, 10 h, 24 h, 48 h) (Krpetić *et al.*, 2011). While the exact same cells are not analysed by TEM as have been measured by the more continuous monitor of fluorescence or optical microscopy, the resolution afforded provides nanoparticle-specific details.

In this paper we review and build on our quantitative description of the tracking of quantum dot, CdSe/ZnS core/shell nanoparticles internalised by U-2 OS cells. We show specific TEM and SBF SEM

analysis of endosome merging and the consequent quantum dot agglomeration process occurring between a 1 h exposure to nanoparticles and a subsequent 24 h incubation period.

## Materials and Methods

### *Sample preparation*

U-2 OS cells were loaded with 10 nM of commercially available Qtracker 705 quantum dots (Invitrogen) as previously described (Summers *et al.*, 2013). The cells exposed to quantum dots were harvested after incubating for 1 h at 37 °C or after a further 24 h incubation in fresh media and placed in fixative (2% glutaraldehyde and 2% formaldehyde in 100 mM PIPES buffer), washed in a buffer, then spun into a pellet, and fixed in 2% osmium tetroxide. Following dehydration by a series of ascending strength alcohols and washing with dry acetone, the specimens were infiltrated with Spurr's resin which was cured at 60 °C for 24 h. For TEM, sections were cut from the polymerized block with a nominal thickness of 100 nm (confirmed by EELS) using an ultramicrotome (Leica Ultracut E) and placed on a copper grid (Agar Scientific). No conventional heavy metal stain (uranyl acetate or lead citrate) was added before imaging.

### *Transmission Electron Microscopy (TEM)*

TEM was conducted on two microscopes: a FEI Tecnai F20 FEG-TEM operating at 200 kV and fitted with a Gatan Orius SC600A CCD camera and a JEOL 2100 TEM operating at 120 kV and fitted with a Gatan Orius SC1000 and a Gatan imaging filter (Tridium). Energy filtered elemental maps were collected using a 3 window approach with the Cd  $M_{4,5}$ -edge collected using 30 eV windows (pre-edge windows centred at 354 and 384 eV and post edge window centred at 469 eV) and the S  $L_{2,3}$ -edge collected using 10 eV windows (pre-edge windows centred at 145 and 155 eV and post edge window centred at 205 eV).

### *Serial Block Face Scanning Electron Microscopy (SBF SEM)*

SBF SEM was conducted using a Gatan 3View system installed on a FEI Quanta 250 FEG operating at an accelerating voltage of 3.8 kV and with a water vapour pressure of 0.64 Torr (85 Pa). The ultramicrotome inside the SEM was used to cut sections from the same polymerized blocks of fixed cells used for TEM at nominal slice thicknesses of 100 nm, with serial backscattered imaging of the exposed block face recorded an area of approximately 70  $\mu\text{m} \times 70 \mu\text{m}$  with a pixel size of 17  $\times$  17 nm, a 15  $\mu\text{s}$  dwell time, a 30  $\mu\text{m}$  objective aperture inserted, and at the manufacturer's spot size setting of 3.5. The image stack was compiled and analysed using three imaging software packages: Gatan Digital Micrograph, Fiji (Schindelin *et al.*, 2012) and Imaris.

### *Stochastic endosome merging model*

The number of quantum dots per endosome,  $x$ , was imaged by TEM and quantified using MATLAB scripts following the identification of 625 and 391 membrane bound vesicles in polymerised cell sections following a 1 h exposure to nanoparticles and a subsequent 24 h incubation period respectively. These numbers were obtained by identification and quantification of all vesicles containing quantum dots within sections of 102 different cells imaged at each exposure/incubation.

Merging or fusion of endosomes and subsequent aggregation of the quantum dots within endosomes was modelled, over the examined time period, by a stochastic process, using the following steps:

- An endosome  $u$  ( $u \in X_1$ ) is chosen at random from the measured set  $X_1$  (subscript denotes 1 h post quantum dot load).
- The number of fusion events  $N$  and the corresponding number of quantum dots per vesicle,  $x$  of the fusing endosomes  $v$  ( $v \in X_1$ ) over the period  $\tau$  is stochastically determined from a Poisson distribution with rate parameter  $\lambda$ .
- A simple minimisation algorithm is employed to optimise the magnitude of  $\lambda$  (Walton *et al.*, 2011) to minimise the L2-norm between the cumulative distribution of the collected and simulated data (Brown *et al.*, 2014).

## Results and Discussion

### *Confirmation of uptake and internalisation of quantum dots*

Our previous analysis of the Qtracker 705 quantum dots has confirmed the crystalline form of the nanoparticles, approximately 10 nm in length (Hondow *et al.*, 2012). The organic coating, composed of arginine-rich targeting peptides conjugated to biotin bonded to streptavidin, is not directly imaged by conventional TEM, however it enables cellular internalisation and endosomal compartmentalisation of the quantum dots, evidence of which can be imaged by TEM (Hondow *et al.*, 2012). It has been previously shown that arginine-rich peptides can lead to cellular uptake via macropinocytosis (Nakase *et al.*, 2004), and similar quantum dots coated with carboxylic acid groups were taken up into human mammary cells by clathrin-mediated endocytosis (Xiao *et al.*, 2010). For U-2 OS cells, quantum dot loadings of up to 10 nM (the concentration used in this study) produce no discernible effect on cell function or longevity (Errington *et al.*, 2010, Summers *et al.*, 2011).

When processing the sample for TEM no additional heavy metal stains were used, with contrast in the cell generated by the osmium containing fixative staining lipid-rich membranes. This sample preparation protocol still enables important cellular features, such as the nucleus, to be identified, as well as the small, high atomic number quantum dots (Figure 1 (a)). As expected, higher magnification imaging shows the particles are membrane bound (Figure 1 (b)), presumably in endosomes or lysosomes, though membrane morphology cannot be used to distinguish between these (Mühlfeld *et al.*, 2007). We suggest because of both the short exposure (1 h) and the intracellular location (near the cell membrane) that these quantum dots are present in an early endosome (Xiao *et al.*, 2010). EDX spot analysis has confirmed that the composition of the dots is broadly unaltered when taken up by U-2 OS cells (Hondow *et al.*, 2014), *i.e.* the analysis is consistent with the expected composition of the CdSe/ZnS dots (Lin *et al.*, 2009, Yang *et al.*, 2007). Lin *et al.* (2009) and Yang *et al.* (2007) measure a largely Cd rich core by ICP-MS, and consequently we have used EFTEM elemental mapping of Cd, in addition to S from the shell, to confirm the location of quantum dots inside the cell (Figure 1 (c) and (d)). Previous concerns expressed by Mühlfeld *et al.* and Rothen-Rutihäuser *et al.* regarding distinguishing electron dense nanoparticles from staining-artefacts due to sample preparation will be limited in this case to osmium staining due to a lack of

post-processing heavy metal stain, but EFTEM analysis eliminates any uncertainty about the intracellular location of dots.

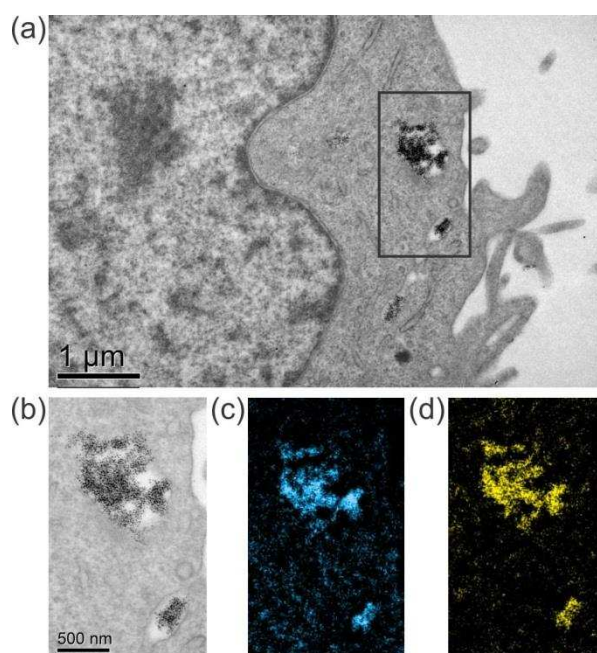


**Figure 1.** TEM and EFTEM imaging of a U-2 OS cell with internalised quantum dots; (a) TEM image; (b) zero-loss image from the area indicated in (a); (c) Cd  $M_{4,5}$ -edge map; (d) S  $L_{2,3}$ -edge map.

The uptake of these quantum dots by U-2 OS cells has been examined using both imaging flow cytometry (Summers *et al.*, 2011) and TEM imaging (Summers *et al.*, 2013). Imaging flow cytometry allows the tracking of fluorescent nanoparticle loaded vesicles, and application to these quantum dots has demonstrated both an initial, highly variable cell loading (that can be fitted by an over-dispersed Poisson probability distribution) and how the cell loading changes over a 24 h period in which some 80% of the cells are expected to have undergone division (Summers *et al.*, 2011). The inheritance of the nanoparticle loaded vesicles after mitosis showed a marked asymmetry in the partitioning of fluorescence between daughter cells. A full interpretation of this required TEM analysis because it has the spatial resolution to examine cellular uptake at the nanoparticle level; the dividing cells separate the endosomes in approximately equal fractions but it is the quantum dot loading of the endosomes that is highly variable (Summers *et al.*, 2013).

TEM of 102 cells within one thin section of a polymerised pellet of cells exposed to the same dose of quantum dots resulted in imaging of all membrane-bound quantum dots within each cell section (Summers *et al.*, 2013). The distribution of vesicles containing quantum dots per cell obtained by TEM imaging differs from that measured by imaging flow cytometry (Summers *et al.*, 2011) for two reasons: first, only a thin cell section was imaged by TEM, and secondly, the TEM can resolve vesicles containing as few as one quantum dot, a level not detectable by (optical) imaging flow cytometry.

This combination of high-resolution, but low-throughput TEM imaging of individual quantum dots and high-throughput fluorescence measurements by imaging flow cytometry offered an avenue to the quantification of dose at the nanoparticle level (Summers *et al.*, 2013). To achieve this, thin

section TEM data had to be related to the whole cell volume and this was achieved using serial block face scanning electron microscopy (SBF SEM). 3-D reconstruction of whole U-2 OS cells exposed to quantum dots by SBF SEM showed agglomerates of nanoparticles both attached to the cell membrane (*i.e.* outside the cell) and internalised within membrane-bound vesicles (Summers *et al.*, 2013). This 3-D analysis was essential to link the high resolution 2-D TEM to the statistically relevant imaging flow cytometry to measure the quantum dot dose.

We have conducted SBF SEM on the same pellet used to produce TEM thin sections of cells exposed to quantum dots for 1 h, *i.e.* with no additional staining required to image the electron dense quantum dots, contrary to the protocol suggested in previous studies (Denk & Horstmann, 2004, Hughes *et al.*, 2013). While individual nanoparticles can no longer be resolved, the quantum dot-filled membrane-bound vesicles can be easily identified (Figure 2 (a)). It has been shown that sectioning in SBF SEM can be reduced to a thickness as low as 25 nm (Friedrich *et al.*, 2013), however we chose to match the SBF SEM section thickness to that analysed in the TEM (100 nm), enabling the collection of a data set of comparable sections. Furthermore, the imaging conditions used for SBF SEM (3.8 kV) were set to ensure that the estimated, maximum backscattered electron emission depth (of  $\sim 70$  nm) was just less than the section thickness (Summers *et al.*, 2013).

It is possible to identify all areas containing quantum dots in a single image slice or cell section from an SBF SEM data set of a cell (Figure 2 (a). For the whole cell view Figure 2 (b) and SI; movie file). Segmenting the quantum dot areas in this, and all other images in the 3-D data set (Figure 2 (c and d) and SI; movie file), suggests that the dots are evenly distributed across the cell slices, both on the individual cell level (Figure 2 (d)) and in a larger population of cells (Summers *et al.*, 2013). The implication of this is that a single 100 nm thick section can be representative of the whole cell. Thus, the use of 100 nm thick sections in both SBF SEM and TEM experiments allowed a direct link between the two data sets, with any one image slice containing approximately 1 % of the total amount of quantum dots internalised in a whole cell (Figure 2 (d); (Summers *et al.*, 2013)). This can then be used to convert the 2-D TEM data to 3-D, enabling calibration of the imaging flow cytometry fluorescence intensity to nanoparticle numbers to provide an estimate of the typical number of quantum dots ( $\sim 2.4$  million) internalised by the U-2 OS cells (Summers *et al.*, 2013).

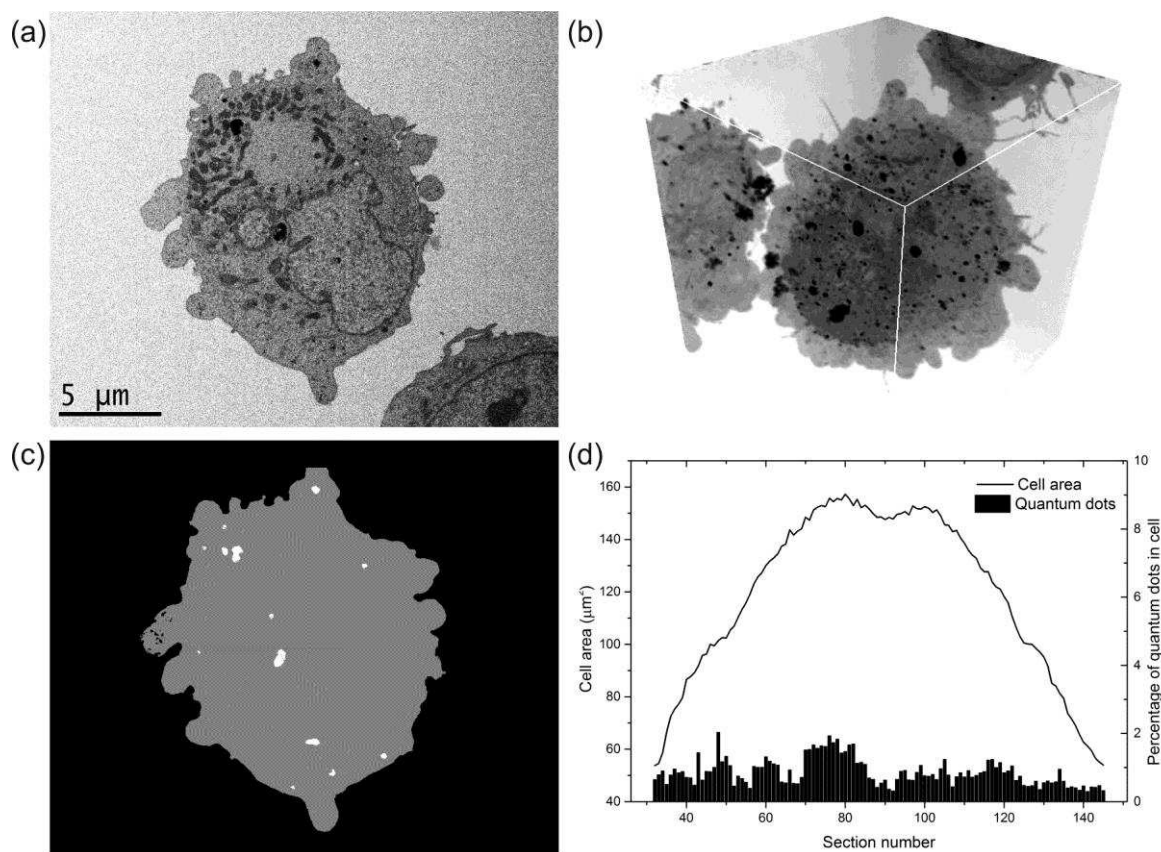


**Figure 2.** Quantification of quantum dots inside a U-2 OS cell after 1 h exposure; (a) one image from a 3-D data set of a full cell acquired by SBF SEM; (b) two-dimensional representation of a 3-D reconstruction of the whole cell imaged in (a) where quantum dots are now visible both on and inside the cell; (c) the image in (a) segmented to identify quantum dot containing areas (white) versus cell (grey); (d) plot comparing the cell area to the percentage of quantum dot containing areas in the cell, showing that the quantum dots are evenly distributed throughout the slices of the cell. (Movies of the cell and segmented cell are available in the SI).

Both the 3-D SBF SEM reconstruction and TEM imaging of thin sections of cells indicates that quantum dot uptake is still taking place at the surface of the U-2 OS cells after 1 h exposure (e.g. Figure 3 (a)). Near the cell membrane it is possible that quantum dots that appear to be internalised may actually be in the early stages of endocytosis, and are part of larger agglomerates still connected to the cell surface. While endocytic uptake can be imaged by TEM (Hondow *et al.*, 2012) it is not always easily identified in thin sections; for example Figure 3 shows quantum dots in a variety of locations, some are outside the cell (Figure 3 (b)), presumably in the process of being taken up into the cell at the time of sample processing, while other nearby groups appear to be in membrane bound vesicles (Figure 3 (c)). TEM imaging is limited by a lack of knowledge of what is present in the thin sections cut immediately prior to and following the section being examined. This raises the question of which areas are independent membrane bound vesicles encapsulating quantum dots, and which are part of a larger network of agglomerates which may still be entering the cell, *i.e.* are only partially encapsulated.

SBF SEM analysis revealed several areas similar to that in Figure 3 (b) where quantum dots are still in the process of entering the cell. Reconstruction of the whole cell shows that quantum dot agglomerates are present in more than one microtome slice, and in one case (Figure 3 (d)) an agglomerate is actually  $\sim 1.2 \mu\text{m}$  in length and  $\sim 1.2 \mu\text{m}$  deep, *i.e.* the agglomerate is present in 12 of the 100 nm SBF SEM sections. There are slices where the agglomerate appears to be internalised in the cell (Figure 3 (e)) and other slices where it is apparently just attached to the surface (Figure 3 (f)). Thus 3-D imaging and reconstruction shows which quantum dots are completely and which are incompletely internalised.

SBF SEM imaging of hydroxyapatite nanoparticles being only partially internalised by human monocyte-macrophages has already been reported (Motskin *et al.*, 2011). In this case, extensive amounts of nanoparticles apparently occupied much of the cell volume yet TEM imaging of labyrinth-like membrane structures indicated the possibility of surface connected compartments, which were only confirmed by SBF SEM. Here, we simply suggest that not all of the quantum dots have been completely internalised, due to a combination of short exposure time and high concentration of quantum dots (limiting the available surface for endocytosis to occur). We should also note that SBF SEM is limited by the lower lateral resolution of the SEM as compared to the TEM (Denk & Horstmann, 2004) and is susceptible to sample bias (Elsaesser *et al.*, 2011), however it can still be a valuable indicator of nanoparticle uptake across a whole cell.

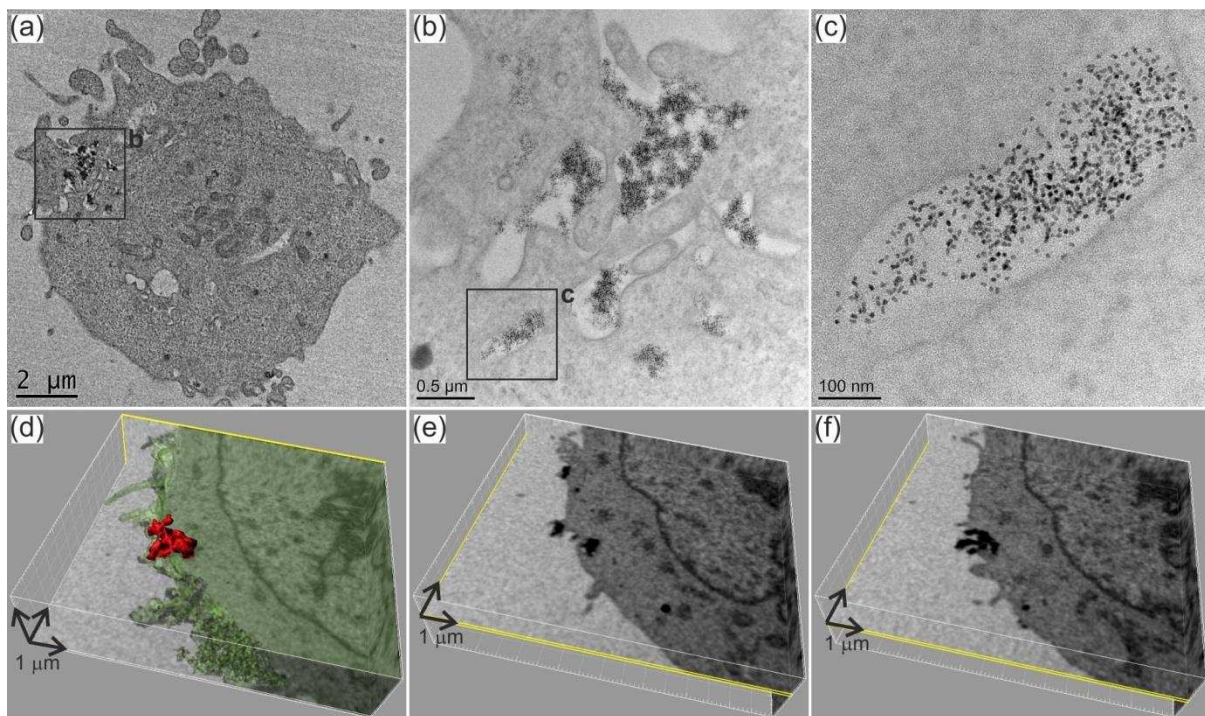


**Figure 3.** (a – c) TEM of a thin section of U-2 OS cells exposed to quantum dots; (a) low magnification image of a cell; (b) higher magnification of the area indicated in (a); (c) higher magnification image of the area indicated in (b) showing agglomerates of quantum dots that appear to be membrane bound.

(d – f) Analysis of a 3-D data set collected across a whole cell by SBF SEM with closer examination of a cropped area. Arrows represent scale bars  $1 \mu\text{m}$  in length. (d) The segmented cell (green) and

agglomerate of quantum dots (red) overlaid on an SBF SEM image slice showing the agglomerate is only in the process of being taken up into the cell; (e) an image slice from the SBF SEM stack which suggests that the agglomerate is two separate agglomerates, one internalised and one on the cell surface; (f) a subsequent slice from the same SBF SEM image stack where it is clear that only one agglomerate is in the process of entering the cell. (Movies of this cropped area of the cell are available in the SI).

### *Intra-cellular processing and agglomeration of quantum dots*

As already stated, 102 cells within a thin slice of a pellet of cells exposed to quantum dots for 1 h were imaged by TEM, producing a data set of 625 vesicles, where the number of quantum dot nanoparticles per vesicle was quantified using automated procedures in MATLAB (Brown *et al.*, 2014, Summers *et al.*, 2013). This vesicular uptake is presumably to endosomes, however it is not possible to establish the exact cellular uptake mechanism via TEM imaging (Mühlfeld *et al.*, 2007). In addition, it has been previously acknowledged that it is difficult to identify a specific entry mechanism as most operate simultaneously and different sized constructs may be taken up by different mechanisms (Canton & Battaglia, 2012), and we have previously shown that these quantum dots do agglomerate to produce a large range of sizes (Figure 4 and (Hondow *et al.*, 2012)).

Recently we have reported a mathematical model that links the quantum dot agglomeration state measured in the cell delivery media to the uptake into membrane bound vesicles of U-2 OS cells following the 1 h exposure (Figure 4 (a)) (Brown *et al.*, 2014). This was achieved by construction and validation of a data-driven, statistical transfer function, enabling modelling of the dynamic properties of nanoparticle agglomeration during endocytosis *i.e.* demonstration of how agglomerates traverse a membrane through a process of inter-agglomerate merging events at the cell surface and endocytic encapsulation operating over a typical time interval of  $\sim 60$  s, which is consistent with that reported previously via high-resolution optical microscopy techniques (Ehrlich *et al.*, 2004, Hansen *et al.*, 1992).

The exposure of U-2 OS cells to the same quantum dot dose for 1 h but then incubated at 37 °C in fresh media for 24 h produces a different data set. Similar to the sample exposed for 1 h, removal of any free quantum dots by washing the cells with fresh media before the incubation period allows this to be simply an examination of what happens to the quantum dots already internalised, or attached to the cellular surface (and presumably undergoing internalisation, Figure 3). Again, 102 cells within one thin resin section of the 24 h incubated cell pellet were imaged by TEM and all membrane bound quantum dots identified and quantified (391 vesicles). Between the 1 and 24 h period, the number of quantum dots per vesicle increases by an order of magnitude (Figure 4 (a), (d) and (e)). The cumulative frequencies of the number of quantum dots per vesicle,  $x$ , at the two distinct time points confirms that on average vesicles in the 24 h dataset ( $F_{24}$ ) have accrued quantum dots compared to those in the 1 h dataset ( $F_1$ ) *i.e.*  $F_1(x) \rightarrow F_{24}(x)$  over the  $\tau = 23$  h period between TEM measurements (Figure 4 (b)).

To model, and therefore enable prediction of, this increase in quantum dots we have applied a stochastic process. Within this, the number of fusion events,  $N$ , that an endosome,  $u$  (chosen at random from the measured set  $X_1$ ), will undergo during the time period,  $\tau$ , is stochastically

determined from a Poisson distribution (Figure 4 (b) inset). The value of the rate parameter  $\lambda$ , the only fitting parameter of the stochastic agglomeration process was optimised using a simple minimisation algorithm (Walton *et al.*, 2011), and determined to be  $1.8 \text{ hr}^{-1}$  (the corresponding model cumulative distribution  $F_{24}^S(x)$  is displayed in Figure 4 (b) by the blue diamonds and curve). This is in agreement with a live-cell study which has shown that endosomal cargo concentrates in progressively fewer and larger endosomes (Rink *et al.*, 2005), despite the debate regarding the precise processing of endocytic compartments (Canton & Battaglia, 2012). Certainly correlative light and electron microscopy has shown coupling and direct fusion events lead to the mixing of endosome and lysosome content (Bright *et al.*, 2005).

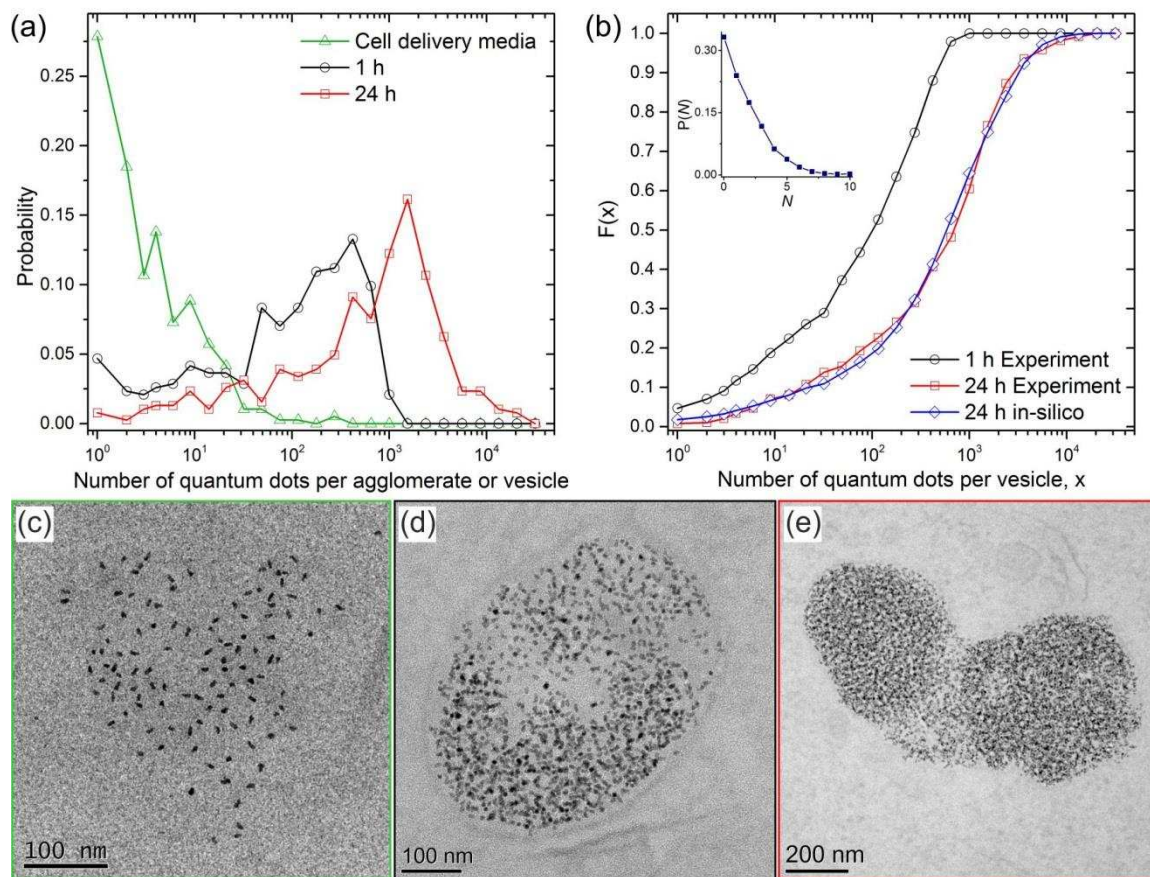


**Figure 4.** (a) Measured probability densities for the number of quantum dots per agglomerate in the cell culture media outside the cell (green curve with triangle markers), the number of quantum dots per vesicle inside U-2 OS cells at 1 h exposure (black curve with circle markers) and after 24 h incubation respectively (red curve with square markers). (b) Comparison of the cumulative distribution functions (CDFs) associated with the number of quantum dots per agglomerate/vesicle measured experimentally and that predicted stochastically. The black curve with circle markers and the red curve with square markers are the CDFs of the measured data at 1 h in media and 24 h post NP load within endosome compartments respectively (*i.e.*  $F_1(x)$  and  $F_{24}(x)$ ). The blue curve with diamond markers is the optimised ( $\lambda = 1.8 \text{ hr}^{-1}$ ) CDF predicted stochastically,  $F_{24}^S(x)$ . A two-sample Kolmogorov-Smirnov test on  $F_{24}(x)$  and  $F_{24}^S(x)$  does not reject the null hypothesis at a significance level of 1% ( $p$ -value of 0.999). Inset graph shows the Poisson distribution  $P(N)$  used to translate

$F_1(x)$  to  $F_{24}^S(x)$ . (c) TEM image of a quantum dot agglomerate present in cell delivery media. (d) TEM image of a membrane bound vesicle containing quantum dots after 1 h exposure. (e) TEM image of a larger membrane bound vesicle containing an increased number of quantum dots after 1h exposure followed by 24 h incubation.

We have also examined the cells incubated for 24 h by SBF SEM of the same resin pellet used to produce TEM thin sections. Similar to the 1 h sample (Figure 2), the quantum dot filled membrane bound vesicles can be identified, segmented and quantified (Figure 5 and SI; movie files). In contrast to the 1 h sample, it is evident that the quantum dots are no longer evenly distributed throughout the cross section of the cell, instead larger agglomerates can be seen towards the centre (Figure 5). Thus, the SBF SEM results broadly agree with the work of Rink *et al* who found that endosomal cargo migrates from the cell periphery to the centre of the cell over time, resulting in larger, centralised endosomes. The perinuclear positioning of the vesicles also suggests directed, maturation to late endosomes or lysosomes (Ferrari *et al.*, 2014). It also dismisses quantitative comparison to other models, such as the entry fusion exit model (Foret *et al.*, 2012). Ultimately, the SBF SEM results suggest we have sufficient sampling by TEM (102 cells in a TEM thin section) to apply the stochastic endosome agglomeration model to predict that endosome fusion is a Poisson (random) driven merging process. We should note that this observation of endocytically compartmentalised quantum dot agglomerates moving to the centre of the cell is specific to Qtracker 705 quantum dots and U-2 OS cells. We have however shown a microscopical framework for the detection, quantification and prediction of quantum dot loads inside any cells at the scale of the individual quantum dot. This is especially important, as nanoparticle agglomerates in general are still often measured in terms of sizes rather than number yet it is the number of nanoparticles that are the fundamental unit of dose (Albanese & Chan, 2011, Brandenberger *et al.*, 2010). Future work will be aided by stereological sampling of cells, potentially examining some of the many variables that can be altered such as cell type, nanoparticle type, nanoparticle surface coating, concentration or applied exposure dose of nanoparticles.

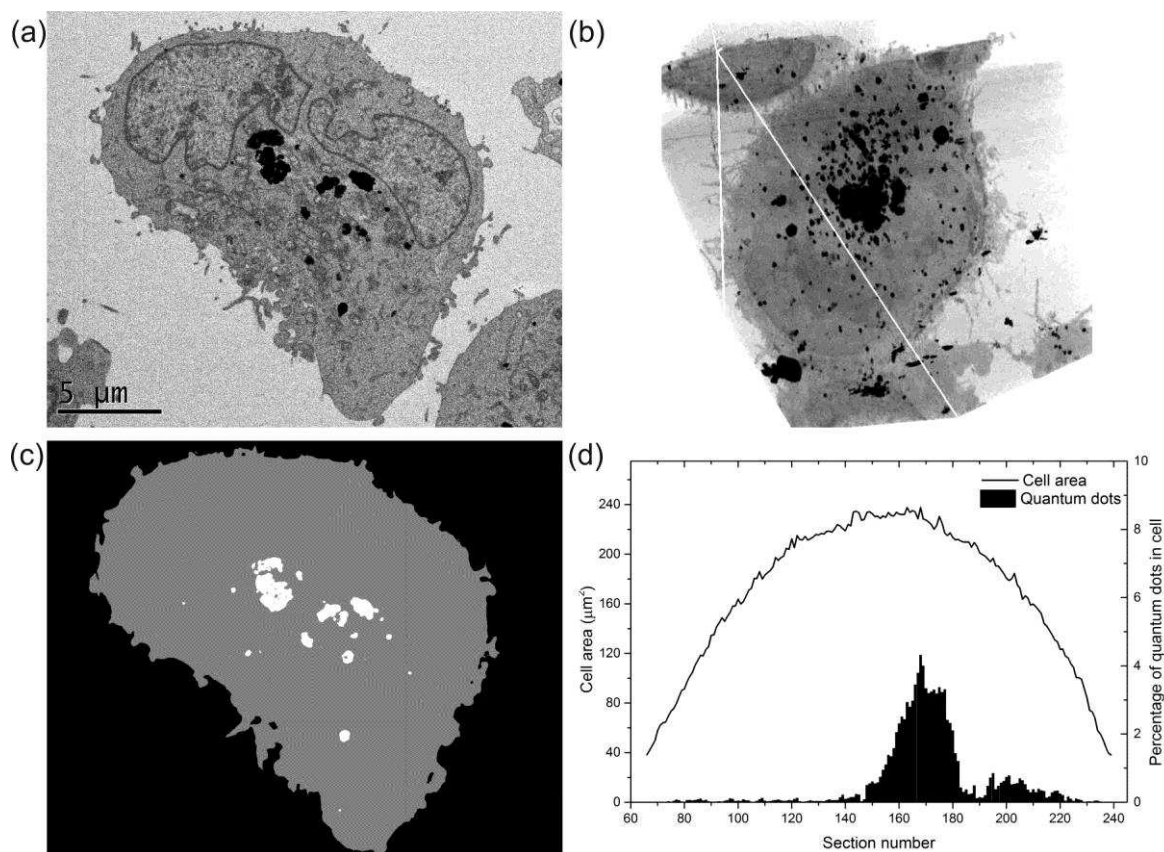


**Figure 5.** Quantification of quantum dots inside a U-2 OS cell after 1 h exposure and 24 h incubation; (a) one image slice from a 3-D data set of a full cell acquired by SBF SEM; (b) two-dimensional representation of a 3-D reconstruction of the whole cell imaged in (a) where the significant majority of quantum dots are visible in the perinuclear region of the cell; (c) the image slice in (a) segmented to allow quantification of cell (grey) versus quantum dot (white) areas; (d) plot comparing the cell area to the percentage of quantum dots in the cell, showing that the quantum dot segments are no longer spread throughout the cell but rather are large and pushed to the centre. (Movies of the cell and segmented cell are available in the SI).

## Conclusions

Analytical electron microscopy is a vital characterisation tool in the development of nanoparticles for biomedical applications. It can be used to assess cellular uptake and for the development of a framework for data driven modelling and prediction of an internalised nanoparticle dose and how that evolves over time.

We have shown that with appropriate sample preparation, the location and composition of quantum dots taken up by U-2 OS cells can be identified and confirmed using analytical electron microscopy. Extensive TEM imaging, in which individual quantum dots can be counted, has been conducted on samples prepared after different incubation periods, allowing for the development of models to predict the evolution of quantum dot agglomeration state from dispersion in cell culture media to initial cellular uptake through processing to late endosomes or lysosomes.

SBF SEM is particularly useful in these nanomedicinal studies because of the capacity to collect 3-D image sets across whole cells. Although not operating at a resolution to identify individual quantum dots, we have used comparable slice thicknesses to TEM sectioning for cross-correlation to TEM imaging at the required resolution and have determined that after 1 h exposure vesicles containing quantum dots are evenly distributed across the cell, such that one thin section is representative of any part of the cell. After 24 h incubation however, vesicles containing significantly larger numbers of quantum dots are identified closer to the centre of cells, consistent with an endosome merging process in operation.

## Acknowledgments

This work was supported by the Engineering and Physical Sciences Research Council, U.K. under Grants EP/H008578/1 (Leeds) and EP/H008683/1 (Swansea). NH is supported by an AXA research fellowship. AGM is employed by Gatan UK, which makes the 3View attachment for SBF SEM. He does not hold shares in Roper Industries Inc., the parent company of Gatan.

We acknowledge A. Warley, K. Brady, and F. Winning (Centre for Ultrastructural Imaging, King's College, London, U.K.) for pelleting and sectioning the cells for TEM. We thank Neil Wilkinson, of Gatan UK, for help with image processing. The Wellcome Trust Centre for Cell-Matrix Research, University of Manchester, is supported by core funding from the Wellcome Trust [grant number 088785/Z/09/Z]. We acknowledge the assistance of Professor Martin Saunders and the facilities of the Australian Microscopy & Microanalysis Research Facility at the Centre for Microscopy, Characterisation & Analysis, The University of Western Australia, a facility funded by the University, State and Commonwealth Governments. This facility was accessed using a World Universities Network Research Mobility Grant (University of Leeds).

## References

- Albanese, A. & Chan, W.C.W. (2011) Effect of Gold Nanoparticle Aggregation on Cell Uptake and Toxicity. *ACS Nano*, **5**, 5478-5489.
- Brandenberger, C., Mühlfeld, C., Ali, Z., Lenz, A.-G., Schmid, O., Parak, W.J., Gehr, P. & Rothen-Rutishauser, B. (2010) Quantitative Evaluation of Cellular Uptake and Trafficking of Plain and Polyethylene Glycol-Coated Gold Nanoparticles. *Small*, **6**, 1669-1678.
- Bright, N.A., Gratian, M.J. & Luzio, J.P. (2005) Endocytic Delivery to Lysosomes Mediated by Concurrent Fusion and Kissing Events in Living Cells. *Current Biology*, **15**, 360-365.
- Brown, A. & Hondow, N. (2013) Chapter 4 - Electron Microscopy of Nanoparticles in Cells. *In: Summers, H. (ed.) Frontiers of Nanoscience*. Elsevier: Vol. 5, pp 95-120.
- Brown, M.R., Hondow, N., Brydson, R., Brown, A., Rees, P. & Summers, H.D. (2014) Statistical prediction of nanoparticle delivery: from cell culture media to cell. *Nanotechnology*, Submitted.
- Brown, M.R., Summers, H.D., Rees, P., Chappell, S.C., Silvestre, O.F., Khan, I.A., Smith, P.J. & Errington, R.J. (2010) Long-Term Time Series Analysis of Quantum Dot Encoded Cells By Deconvolution of the Autofluorescence Signal. *Cytometry A*, **77A**, 925-932.
- Canton, I. & Battaglia, G. (2012) Endocytosis at the nanoscale. *Chemical Society Reviews*, **41**, 2718-2739.

- De Jong, W.H. & Borm, P.J.A. (2008) Drug delivery and nanoparticles: Applications and hazards. *Int. J. Nanomed.*, **3**, 133-149.
- Denk, W. & Horstmann, H. (2004) Serial block-face scanning electron microscopy to reconstruct three-dimensional tissue nanostructure. *PLoS Biol.*, **2**, e329.
- Doane, T.L. & Burda, C. (2012) The unique role of nanoparticles in nanomedicine: imaging, drug delivery and therapy. *Chem. Soc. Rev.*, **41**, 2885-2911.
- Ehrlich, M., Boll, W., Van Oijen, A., Hariharan, R., Chandran, K., Nibert, M.L. & Kirchhausen, T. (2004) Endocytosis by random initiation and stabilization of clathrin-coated pits. *Cell*, **118**, 591-605.
- Elsaesser, A., Barnes, C.A., McKerr, G., Salvati, A., Lynch, I., Dawson, K.A. & Howard, C.V. (2011) Quantification of nanoparticle uptake by cells using an unbiased sampling method and electron microscopy. *Nanomedicine*, **6**, 1189-1198.
- Errington, R.J., Brown, M.R., Silvestre, O., Njoh, K.L., Chappell, S.C., Khan, I., Rees, P., Wilks, S.P., Smith, P.J. & Summers, H.D. (2010) Single cell nanoparticle tracking to model cell cycle dynamics and compartmental inheritance. *Cell Cycle*, **9**, 121-130.
- Etheridge, M.L., Campbell, S.A., Erdman, A.G., Haynes, C.L., Wolf, S.M. & McCullough, J. (2013) The big picture on nanomedicine: the state of investigational and approved nanomedicine products. *Nanomed-Nanotechnol*, **9**, 1-14.
- Ferrari, R., Lupi, M., Falcetta, F., Bigini, P., Paoletta, K., Fiordaliso, F., Bisighini, C., Salmona, M., D'Incalci, M., Morbidelli, M., Moscatelli, D. & Ubezio, P. (2014) Integrated multiplatform method for in vitro quantitative assessment of cellular uptake for fluorescent polymer nanoparticles. *Nanotechnology*, **25**, 045102.
- Foret, L., Dawson, J.E., Villasenor, R., Collinet, C., Deutsch, A., Bruschi, L., Zerial, M., Kalaidzidis, Y. & Julicher, F. (2012) A General Theoretical Framework to Infer Endosomal Network Dynamics from Quantitative Image Analysis. *Current Biology*, **22**, 1381-1390.
- Friedrich, R., Genoud, C. & Wanner, A.A. (2013) Analyzing the structure and function of neuronal circuits in zebrafish. *Front. Neural Circuits*, **7**, 71.
- Hansen, S.H., Sandvig, K. & van Deurs, B. (1992) Internalization efficiency of the transferrin receptor. *Exp. Cell. Res.*, **199**, 19-28.
- Hashimoto, T., Thompson, G.E., Curioni, M., Zhou, X.R. & Skeldon, P. (2013) Three dimensional imaging of light metals using serial block face scanning electron microscopy (SBFSEM). *Mater. Sci. Forum*, **765**, 501-505.
- Hondow, N., Brydson, R. & Brown, A. (2014) The use of transmission electron microscopy in the quantification of nanoparticle dose. *J. Phys. Conf. Proc.*, **522**, 012055.
- Hondow, N., Brydson, R., Wang, P., Holton, M.D., Brown, M.R., Rees, P., Summers, H.D. & Brown, A. (2012) Quantitative characterization of nanoparticle agglomeration within biological media. *J. Nanopart. Res.*, **14**, 977.
- Hughes, L., Hawes, C., Monteith, S. & Vaughan, S. (2013) Serial block face scanning electron microscopy—the future of cell ultrastructure imaging. *Protoplasma*, 1-7.
- Jaiswal, J.K., Mattoussi, H., Mauro, J.M. & Simon, S.M. (2003) Long-term multiple color imaging of live cells using quantum dot bioconjugates. *Nat. Biotech.*, **21**, 47-51.
- Jamieson, T., Bakhshi, R., Petrova, D., Pocock, R., Imani, M. & Seifalian, A.M. (2007) Biological applications of quantum dots. *Biomaterials*, **28**, 4717-4732.
- Kim, B.Y.S., Rutka, J.T. & Chan, W.C.W. (2010) Nanomedicine. *New Engl. J. Med.*, **363**, 2434-2443.
- Koo, O.M., Rubinstein, I. & Onyuksel, H. (2005) Role of nanotechnology in targeted drug delivery and imaging: a concise review. *Nanomed-Nanotechnol*, **1**, 193-212.
- Krpetić, Ž., Saleemi, S., Prior, I.A., Sée, V., Qureshi, R. & Brust, M. (2011) Negotiation of Intracellular Membrane Barriers by TAT-Modified Gold Nanoparticles. *ACS Nano*, **5**, 5195-5201.
- Leis, A., Rockel, B., Andrees, L. & Baumeister, W. (2008) Visualizing cells at the nanoscale. *Trends Biochem. Sci.*, **34**, 60-70.

- Lin, C.-H., Chang, L.W., Chang, H., Yang, M.-H., Yang, C.-S., Lai, W.-H., Chang, W.-H. & Lin, P. (2009) The chemical fate of the Cd/Se/Te-based quantum dot 705 in the biological system: toxicity implications. *Nanotechnology*, **20**, 215101.
- Michalet, X., Pinaud, F.F., Bentolila, L.A., Tsay, J.M., Doose, S., Li, J.J., Sundaresan, G., Wu, A.M., Gambhir, S.S. & Weiss, S. (2005) Quantum dots for live cells, *in vivo* imaging, and diagnostics. *Science*, **307**, 538-544.
- Motskin, M., Müller, K.H., Genoud, C., Monteith, A.G. & Skepper, J.N. (2011) The sequestration of hydroxyapatite nanoparticles by human monocyte-macrophages in a compartment that allows free diffusion with the extracellular environment. *Biomaterials*, **32**, 9470-9482.
- Mu, Q., Hondow, N.S., Krzemiński, Ł., Brown, A.P., Jeuken, L.J.C. & Routledge, M.N. (2012) Mechanism of cellular uptake of genotoxic silica nanoparticles. *Particle Fibre Toxicol.*, **9**, 29.
- Mühlfeld, C., Rothen-Rutishauser, B., Vanhecke, D., Blank, F., Gehr, P. & Ochs, M. (2007) Visualization and quantitative analysis of nanoparticles in the respiratory tract by transmission electron microscopy. *Particle Fibre Toxicol.*, **4**, 11.
- Nakase, I., Niwa, M., Takeuchi, T., Sonomura, K., Kawabata, N., Koike, Y., Takehashi, M., Tanaka, S., Ueda, K., Simpson, J.C., Jones, A.T., Sugiura, Y. & Futaki, S. (2004) Cellular uptake of arginine-rich peptides: Roles for macropinocytosis and actin rearrangement. *Mol. Ther.*, **10**, 1011-1022.
- Rees, P., Wills, J.W., Brown, M.R., Tonkin, J., Holton, M.D., Hondow, N., Brown, A.P., Brydson, R., Millar, V., Carpenter, A.E. & Summers, H.D. (2014) Nanoparticle vesicle encoding for imaging and tracking cell populations. *Nat Meth*, **11**, 1177-1181.
- Rink, J., Ghigo, E., Kalaidzidis, Y. & Zerial, M. (2005) Rab conversion as a mechanism of progression from early to late endosomes. *Cell*, **122**, 735-749.
- Rothen-Rutishauser, B.M., Schürch, S., Haenni, B., Kapp, N. & Gehr, P. (2006) Interaction of fine particles and nanoparticles with red blood cells visualized with advanced microscopic techniques. *Environ. Sci. Technol.*, **40**, 4353-4359.
- Schindelin, J., Arganda-Carreras, I., Frise, E., Kaynig, V., Longair, M., Pietzsch, T., Preibisch, S., Rueden, C., Saalfeld, S., Schmid, B., Tinevez, J.-Y., White, D.J., Hartenstein, V., Eliceiri, K., Tomancak, P. & Cardona, A. (2012) Fiji: an open-source platform for biological-image analysis. *Nat. Meth.*, **9**, 676-682.
- Shapero, K., Fenaroli, F., Lynch, I., Cottell, D.C., Salvati, A. & Dawson, K.A. (2011) Time and space resolved uptake study of silica nanoparticles by human cells. *Molecular BioSystems*, **7**, 371-378.
- Summers, H.D., Brown, M.R., Holton, M.D., Tonkin, J.A., Hondow, N., Brown, A.P., Brydson, R. & Rees, P. (2013) Quantification of nanoparticle dose and vesicular inheritance in proliferating cells. *ACS Nano*, **7**, 6129-6137.
- Summers, H.D., Rees, P., Holton, M.D., Brown, M.R., Chappell, S.C., Smith, P.J. & Errington, R.J. (2011) Statistical analysis of nanoparticle dosing in a dynamic cellular system. *Nat. Nano.*, **6**, 170-174.
- Walton, S., Hassan, O., Morgan, K. & Brown, M.R. (2011) Modified cuckoo search: A new gradient free optimisation algorithm. *Chaos Soliton. Fract.*, **44**, 710-718.
- Wang, Y. & Chen, L. (2011) Quantum dots, lighting up the research and development of nanomedicine. *Nanomed-Nanotechnol*, **7**, 385-402.
- White, J.G., Southgate, E., Thomson, J.N. & Brenner, S. (1986) The structure of the nervous system of the nematode *caenorhabditis elegans*. *Philos. Trans. Royal Soc. Lond. B*, **314**, 1-340.
- Xiao, Y., Forry, S., Gao, X., Holbrook, R.D., Telford, W. & Tona, A. (2010) Dynamics and mechanisms of quantum dot nanoparticle cellular uptake. *J. Nanobiotechnol.*, **8**, 13.
- Yang, R.S.H., Chang, L.W., Wu, J.-P., Tsai, M.-H., Wang, H.-J., Kuo, Y.-C., Yeh, T.-K., Yang, C.S. & Lin, P. (2007) Persistent tissue kinetics and redistribution of nanoparticles, quantum dot 705, in mice: ICP-MS quantitative assessment. *Environ. Health Persp.*, **115**, 1339-1343.

Zankel, A., Kraus, B., Poelt, P., Schaffer, M. & Ingolic, E. (2009) Ultramicrotomy in the ESEM, a versatile method for materials and life sciences. *J. Microsc.*, **233**, 140-148.